

Article

Adsorption and Its Mechanism of Arsenate in Aqueous Solutions by Red Soil

Min Guo, Lili Shi, Wen Gu and Wenzhu Wu * 

Key Laboratory of Pesticide Environmental Assessment and Pollution Control, Nanjing Institute of Environmental Sciences, Ministry of Ecology and Environment of the People's Republic of China, Nanjing 210042, China; guomin@nies.org (M.G.); sll@nies.org (L.S.); guwen@nies.org (W.G.)

* Correspondence: wwz@nies.org; Tel.: +86-(25)-8528-7202

Abstract: The removal, and its mechanism, of arsenate from aqueous solutions was investigated using Yunnan red soil. A series of adsorption experiments was designed to disclose the effect of key factors (soil types, soil/solution rates, initial arsenate concentrations, and shaking speeds) on the adsorption capacity of Yunnan red soil for arsenate. The soil/solution ratio was optimized as 0.05 g/100 mL to balance the adsorption capacity and removal efficiency. The optimal shaking speed (225 rpm) not only ensured enough contact frequency between the Yunnan red soil and the arsenate, but also reduced the mass transfer resistance. The results from applying an orthogonal array method showed that the most significant factor affecting arsenate removal efficiency was soil type, followed by the soil/solution ratio, contact time, and shaking speed. The IR spectra of the precipitates further confirmed that the metal arsenide was settled by the Yunnan red soil, indicating that the arsenate ion existed on the red soil surface in the form of protonated bidentate surface complexation of $-\text{FeO}_2\text{As}(\text{O})(\text{OH})^-$ and $\text{FeO}_2\text{As}(\text{O})^{2-}$. These results indicate that Yunnan red soil is promising for the removal of arsenate from aqueous solutions; it may thus be suitable as a new adsorbent for arsenate removal during water treatment.

Keywords: soil; As(V); adsorption; water treatment; $\text{L}_9(3^4)$; mechanism



Citation: Guo, M.; Shi, L.; Gu, W.; Wu, W. Adsorption and Its Mechanism of Arsenate in Aqueous Solutions by Red Soil. *Water* **2022**, *14*, 579. <https://doi.org/10.3390/w14040579>

Academic Editors: Dibyendu Sarkar, Rupali Datta, Prafulla Kumar Sahoo and Mohammad Mahmudur Rahman

Received: 20 December 2021

Accepted: 3 February 2022

Published: 14 February 2022

Publisher's Note: MDPI stays neutral with regard to jurisdictional claims in published maps and institutional affiliations.



Copyright: © 2022 by the authors. Licensee MDPI, Basel, Switzerland. This article is an open access article distributed under the terms and conditions of the Creative Commons Attribution (CC BY) license (<https://creativecommons.org/licenses/by/4.0/>).

1. Introduction

Arsenic is a metalloid that is considered to be a dangerous water pollutant throughout the world. It occurs in natural waters in both inorganic and organic forms, with the inorganic form being more toxic than the organic form. Arsenic usually occurs in two valence states: arsenite (As (III)) and arsenate (As (V)) [1]. Arsenic has been listed as a Class A carcinogen by the US Environmental Protection Agency (US EPA) due to its high toxic effects [2], and the US EPA in 2001 adopted a new standard for arsenic in drinking water at 10 µg/L, replacing the old standard of 50 µg/L. Considering its health and toxicological effects, the World Health Organization has revised the maximum contaminant level (MCL) for arsenic in drinking water from 50 to 10 µg/L [3]. Japan and the European Union have complied with the standard of 10 µg/L for arsenic instead of 50 µg/L, which has been used for years [4–6]. China has also set the limit of arsenic concentration in drinking water at 10 µg/L via the China Drinking Water Sanitary Standard (GB5749-2006). However, the current water contamination caused by arsenic is severe, with at least 50 million people in Asia drinking underground water with arsenic concentrations exceeding 50 µg/L [7]. China also faces water contamination problems, from both industrial and natural sources, of enormous proportions. Yunnan Province in southwest China is abundant with mineral resources. The development of the mining industry in recent years has resulted in pollution caused by heavy metals and metalloids becoming increasingly serious. In 2008, the average value of arsenic concentrations in Yangzonghai Lake, Yunnan Province, reached 0.121 mg/L. The water quality of Yangzonghai Lake was identified as inferior grade V, which seriously

affected the production and lives of the local population. Later, Datunhai Lake in Honghe Prefecture, Yunnan Province, was found to have several times the pollution of Yangzonghai Lake, with an arsenic concentration exceeding 96 times the national standards. There are substantial data showing that more than 50% of the lakes in Honghe Prefecture are seriously contaminated by arsenic, and thus require urgent contamination control.

Various treatment methods have been used for the removal of arsenic from water and wastewater, such as chemical oxidation, membrane processes, adsorption, biological methods, ion exchange, and electrocoagulation [8,9]. Adsorption has been recognized as an effective treatment method. It has been observed that arsenate is well adsorbed onto the surface of iron-containing compounds, such as ferric hydroxide, aluminum hydroxide, Fe–Al hydroxide, and manganese dioxide [10–18]. Owing to the complexity of soil composition and structure, the current research on the mechanisms of arsenic sorption in environmental media is still mainly focused on the sorption behaviors of pure minerals or iron-containing compounds; hence, more research is needed on arsenic sorption, especially in soil.

The red soil in Yunnan Province has a high clay content and is rich in Fe and Al oxides; these properties are beneficial for the adsorption of arsenic. Hence, an attempt was made in the present investigations to test the red soil for arsenate adsorption from aqueous solution. In the current study, adsorption equilibrium experiments were conducted under different conditions, which also correspond to the current pollution actuality of Yunnan Province, thus exploring fast, efficient, natural, and harmless arsenic removal technology. The red soil chosen as the sorbent is cheaper than other options and more easily obtained. The red-soil-adsorbed arsenic will sink to the bottom of the lake and thus will not produce large amounts of chemical sludge, which needs further treatment. This technology will have important application value and practical significance for surface water polluted by arsenic, especially for the treatment of arsenic-contaminated lakes in China's southwestern regions.

2. Materials and Methods

2.1. Materials

All reagents used in this study were of analytical grade. Stock solutions of test reagents were prepared in milli Q water. All glassware and sample bottles were soaked in 10% HNO₃ and then rinsed with milli Q water. The resistivity and TOC of milli Q water are 18.2 Ω and <5, respectively. The following reagents were used:

- (1) Sodium arsenate heptahydrate (Na₂HAsO₄·7H₂O) with a purity of 98% was provided by US Alfa Aesar.
- (2) A 1% potassium borohydride (KBH₄) solution was prepared by dissolving 0.2 g of potassium hydroxide in 100 mL milli Q water, and then 1 g of potassium borohydride was added into the solution and mixed fully.
- (3) A 2% hydrochloric acid solution with 10 mL of concentrated hydrochloric acid was diluted to 500 mL with milli Q water. All solutions were prepared using the 2% HCl solution.
- (4) Soils and their characterization.

Six typical types of red soil in the southwest of China were chosen as objects for the experiment: four types of Yunnan red soil, one Jiangxi red soil, and one Guangdong latosol. The essential physiochemical properties are shown in Table 1. These soils were air-dried and passed through a mesh of size 200 for further investigation.

Table 1. The Essential Physiochemical Properties of Six Typical Soils.

Soils	pH	Organic Matter (g/kg)	Soil Physical Sand Content (1~0.01 mm) %	Soil Physical Clay Content (<0.01 mm) %	Fe ₂ O ₃ /%	Al ₂ O ₃ /%
Yunnan red soil 1	6.59	9.3	70.7	29.3	14.04	28.86
Yunnan red soil 2	6.47	9.2	57.3	42.7	10.05	24.48
Yunnan red soil 3	5.93	10.2	60.8	39.2	12.59	26.70
Yunnan red soil 4	5.88	11.9	73.3	26.7	12.86	26.51
Jiangxi red soil	6.24	17.0	87.9	12.1	8.91	18.28
Guangdong latosol	6.55	15.1	59.2	40.8	8.29	18.56

Note: All information was determined by our laboratory.

2.2. Equipment

The equipment used consisted of a PF6 non-dispersive atomic fluorescence spectrometer (Purkinje General, China), a VECTOR-22 infrared spectrometer (Bruker Optics Inc., Ettlingen, Germany), and an E24A-thermostat digital oscillator (New Brunswick Scientific, Edison, NJ, USA).

2.3. Batch Adsorption Studies

Equilibrium experiments of arsenate sorption onto the soils were carried out by batch adsorption with aqueous solutions of As(V). The adsorption studies were launched with six different soils, and then the two best soils were chosen for the following experiment according to the adsorption effect. The reaction vessels were equilibrated in a temperature-controlled shaker under different conditions, including different shaking bath speeds ranging from 50 to 300 rpm, different initial concentrations of arsenate ranging from 0.05 to 2.0 mg/L, and different addition ratios of soils ranging from 0.01 to 0.5 g soils/100 mL to study the adsorption behavior of arsenate in soil.

Yangzonghai Lake is one of the largest plateau lakes in Yunnan Province, China. It is the main water source for agriculture, fisheries, and drinking water for its surrounding areas. The arsenic concentrations in Yangzonghai Lake were found to be three times as high as the maximum allowable concentration (MAC) (0.05 mg/L) of grade III of China's Surface Water Environmental Quality Standards, and approximately 1.5-fold higher than that of grade V according to the field research carried out by our workgroup, which was consistent with a previous investigation [19]. Moreover, the arsenic present in the water was mainly in pentavalent form. Therefore, 0.2 mg/L arsenate aqueous solution was chosen to be the suitable concentration in Sections 3.2 and 3.4.

The residual concentrations of arsenate in the filtrate were determined using a PF6 atomic fluorescence spectrometer (Purkinje General), once filtered.

2.4. Adsorption Mechanism

Infrared spectra of the red soil before and after arsenate adsorption were recorded using a VECTOR-22 infrared spectrometer.

For IR identification, a 150 g sample consisting of red soil and KBr in a ratio of 1/200 was uniformly mixed and then pressed into one piece under a pressure of 10 t/cm² for 1 min. A FT-IR spectrometer was then used to measure the sample spectra values within the range of 4000–400 cm⁻¹.

The analyses by scanning electron microscopy (SEM) image were completed using a Hitachi S-4800 SEM.

2.5. Analytical Methods

Sample pretreatment was carried out with acidified samples of 10% HCl thoroughly mixed with 1% thiourea and 1% ascorbic acid; these were then measured after 30 min.

For the measurement conditions, the negative high voltage on the photomultiplier tube was set to 265 V, the atomization temperature was set to 180 °C, and the lamp current

of the As hollow-cathode lamp was set to 40 mA; 300 and 600 mL/min flow rates of carrier gas and shield gas were set, respectively.

The instrument was calibrated from 1.0 to 20.0 $\mu\text{g/L}$. Other range samples were diluted until results within the calibration range were obtained.

2.6. Orthogonal Analysis

The orthogonal array method was used to determine the optimum levels of factors that affect the removal rates. Selected factors (soil type, soil/solution ratio, contact time, and shaking speed) were studied at three levels. According to an L_9 (3^4) orthogonal array, nine trials with three replications were conducted.

3. Results and Discussions

3.1. Effect of Soil Types on the Adsorption of Arsenate

In any adsorption process, the adsorption material has a significant effect on the treatment efficiency. Therefore, appropriate selection of the red soil is important. Hence, six different red soils were chosen as adsorbents; these soils are non-toxic and comprise high clay, iron oxide, and aluminum oxide.

Six types of red soil (0.5 g) were added to a reaction vessel containing 100 mL of arsenate solution with a concentration of 10 mg/L. The reaction vessels were then equilibrated in a shaking bath at 225 rpm for a period of 10 h. Figure 1 shows the variation in the arsenate removal rate with different red soils. It can be observed from Figure 1 that the removal of all six adsorption reactions increased over time until a steady state was attained after approximately 2 h, and there was no significant change in the pseudo equilibrium concentration after this time until 10 h. The removal of arsenate when using Yunnan red soil (1, 3, and 4) in the aqueous solution increased significantly compared with the other three soils, with removal rates of up to 49.5%, 44.8%, and 44.0%, and with adsorption capacities of 989.2 $\mu\text{g/g}$, 895.1 $\mu\text{g/g}$, and 879.3 $\mu\text{g/g}$, respectively. Studies on arsenic have indicated that hydrous metal oxides, such as ferric hydroxides, ferrihydrite, and goethite, strongly adsorb arsenic. The adsorption rates of arsenate on Yunnan red soil 2, Jiangxi red soil, and Guangdong latosol were low, which may be related to the relatively low content of iron oxide and aluminum oxide in these three soils. The curves in Figure 1 also show rapid arsenate adsorption in the beginning, which may be attributed to the relatively large number of available vacant sites on the soils compared to those of the later hours.

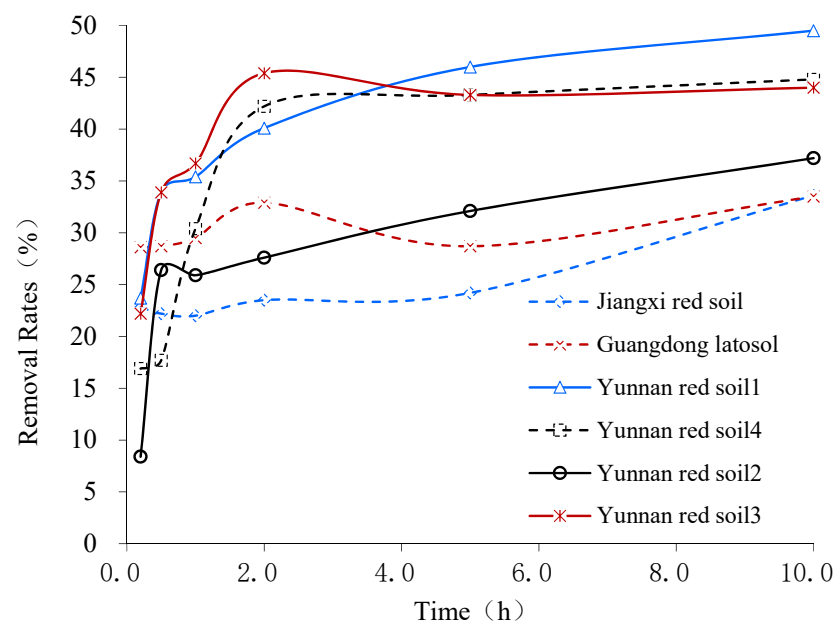


Figure 1. Removal Percentage of As(V) on Different Red Soils.

3.2. Effect of Soil/Solution Ratios

Two soils (Yunnan red soil 1 and 4) with relatively high adsorption capacity were selected for the following experiments.

The sensitivity of As(V) adsorption efficiency to the adsorbent dosage was determined by adding 0.01, 0.02, 0.03, 0.05, 0.1, 0.2, 0.3, and 0.5 g red soil (Yunnan red soil 1 and 4) into 100 mL solutions at a constant test solution As(V) concentration of 0.2 mg/L. The reaction vessels were then equilibrated in a shaking bath at 225 rpm for a period of 2 h. As shown in Figure 2, the adsorption capacity of these two soils all increased with increasing soil/solution ratio. The arsenate adsorption capacity depended profoundly on the soil/solution ratio in the range of 0.01 g/100 mL to 0.05 g/100 mL; the removal rates were 51.1%, 69.2%, 82.2%, and 94.8% (Yunnan red soil 1) and 45.4%, 65.5%, 81.0%, and 93.4% (Yunnan red soil 4) at the soil/solution ratios of 0.01 g/100 mL, 0.02 g/100 mL, 0.03 g/100 mL, and 0.05 g/100 mL, with arsenate adsorption capacities of 1023, 692, 548, and 379 (Yunnan red soil 1) and 908, 655, 540, and 374 (Yunnan red soil 4) µg/g. The removal rates increased with increasing soil dosage, but the removal increased at 0.05 g dosage and leveled off after that point. This behavior implies that the sorption depends on the availability of binding sites.

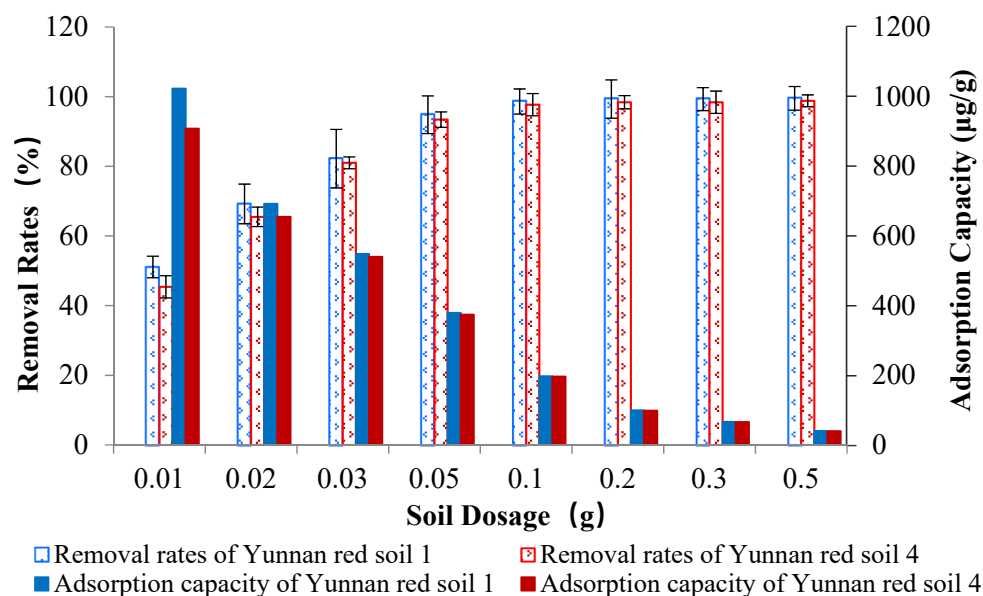


Figure 2. Removal Percentage of As(V) at Different Soil/solution Ratios.

3.3. Effect of Initial Arsenate Concentration

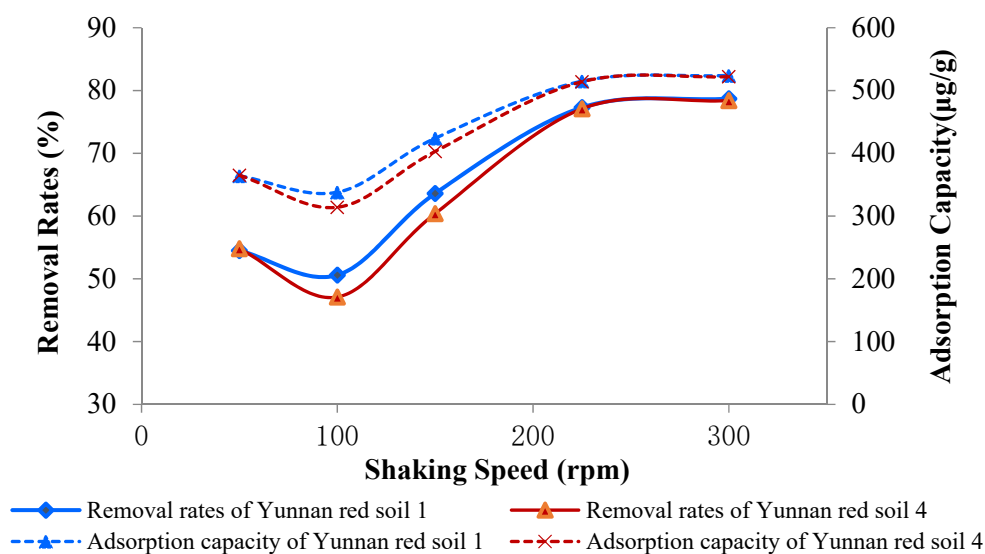
Most surface, ground, and industrial waste waters contain different concentration levels of arsenate; therefore, arsenate concentrations in the range of 0.05 to 2.0 mg/L were chosen for the present findings to match with the natural water system. The adsorption capacity of two different red soils (Yunnan red soil 1 and Yunnan red soil 4) increased with increasing initial arsenate concentration (Table 2). This may be an outcome of the increase in driving force due to the concentration gradient building up between the surface of the red soil and the arsenate solution [20]. Table 2 also reveals that the removal rates of arsenate decreased with increasing initial arsenate concentration. This may be attributed to the fixed quantity of red soils being used during the course of the adsorption process. At the same time, the arsenate adsorption capacity of Yunnan red soil 4 was slightly larger than that of Yunnan red soil 1 at each initial concentration, which indicated that the pH and organic matter content of the soil are also important factors in the adsorption progress.

Table 2. Effect of Initial Arsenate Concentration on the Sorption of Arsenate.

Initial Concentration (mg/L)	Yunnan Red Soil 1			Yunnan Red Soil 4		
	Removal Rate (%)	RSD (%)	Adsorption Capacity ($\mu\text{g/g}$)	Removal Rate (%)	RSD (%)	Adsorption Capacity ($\mu\text{g/g}$)
0.05	95.1	4.0	158.5	95.5	5.7	159.1
0.1	92.2	5.6	307.3	93.2	8.1	310.7
0.2	79.5	5.4	529.8	82.5	5.2	550.3
0.5	58.8	3.6	979.2	59.3	0.7	987.7
1.0	41.6	0.9	1387.3	42.8	1.8	1427.7
2.0	20.8	3.7	1389.2	24.6	0.1	1637.1

3.4. Effect of Shaking Speed on the Removal of Arsenate

The adsorption was influenced by the mixing conditions of the reaction system. Because the batch adsorption reactions took place in a shaker, the shaking speeds were investigated as an influencing factor. From Figure 3, the adsorption capacities of Yunnan red soil 1 and Yunnan red soil 4 all fell in the range of 50 rpm to 100 rpm. An optimal shaking speed ensured sufficient contact frequency between the sorbent and the adsorbate, which was helpful to improve the adsorption capacity of the sorbent. However, a higher shaking speed might decrease the adsorption capacity by producing a strong shearing effect [21]. Once the shaking speed was over 100 rpm, the removal rates of arsenate increased with increasing shaking speed and reached a peak at 225 rpm, then the adsorption capacity of these two red soils increased slightly with ascending shaking speed. Therefore, a shaking speed of 225 rpm was fixed in the relevant experiments.

**Figure 3.** Effect of the Shaking Speed on the Adsorption Process.

3.5. Optimization of the Factors Affecting Arsenate Removal by Orthogonal Array

Experiments were performed with the soil types of Yunnan red soil 1, 2, and 4; soil/solution ratios of 0.025 g/100 mL, 0.030 g/100 mL, and 0.035 g/100 mL; contact times of 15, 30, and 45 min; and shaking speeds of 200, 225, and 250 rpm. The influences of these factors on the removal rate were determined using the maximum difference method (Table 3).

Table 3. The L_9 (3^4) Orthogonal Array Experimental Design and Arsenate Removal Efficiency As Response.

No.	A *. Soil Type	B *. Soil/Solution Ratio (g/mL)	C *. Contact Time (min)	D *. Shaking Speed (rpm)	Removal Rate (%)
1	1 (Yunnan red soil 1)	1 (0.025/100)	1 (15)	1 (200)	64.1
2	1	2 (0.030/100)	2 (30)	2 (225)	76.5
3	1	3 (0.035/100)	3 (45)	3 (250)	84.8
4	2 (Yunnan red soil 2)	1	2	3	47.0
5	2	2	3	1	55.8
6	2	3	1	2	54.2
7	3 (Yunnan red soil 4)	1	3	2	70.7
8	3	2	1	3	69.6
9	3	3	2	1	78.8
k1	225.4	181.8	187.9	198.7	
k2	157.0	201.9	202.3	201.4	
k3	219.1	217.8	211.3	201.4	
K1	75.1	60.6	62.6	66.2	
K2	52.3	67.3	67.4	67.1	
K3	73.0	72.6	70.4	67.1	
R (max-min)	22.8	12.0	7.8	0.9	

* the key factors.

The final removal efficiencies of arsenate from aqueous solution by red soil are presented in Table 3. The range[®], calculated from the results of the orthogonal experiment, indicates that soil type has the largest effect on removal rate, followed by soil/solution ratio, contact time, and shaking speed.

3.6. Adsorption Mechanism of the Red Soils

Many studies have shown that iron and aluminum in soil play an important role in arsenic adsorption [22]. Arsenate can form insoluble arsenide with iron and aluminum cations and produce co-precipitation with amorphous iron and aluminum hydroxide. The more amorphous Fe and Al oxides contained in the soil, the stronger the arsenic adsorption capacity [23,24]. Arsenic can be fixed on the surface of metal oxide through specific adsorption and non-specific adsorption. Specific adsorption refers to the entrance of anions into the metal atom coordination shell on the oxide surface to re-coordinate with the ligand hydroxyl or hydrated to combine on the solid surface directly through covalent bonding or coordinate bonding [25,26]. Spectroscopic studies have confirmed that both As(III) and As(V) may form inner-sphere complexes on the surfaces of (hydr)oxides and clay minerals through ligand exchange with OH and OH^{2+} surface functional groups [27]. In situ, Raman and Fourier transform infrared (FTIR) spectroscopic methods, combined with sorption techniques, electrophoretic mobility measurements, and surface complexation modeling, were used by Goldberg [28] to study the interaction of As(III) and As(V) with amorphous oxide surfaces, and the results showed that arsenate formed inner-sphere surface complexes on both amorphous Al and Fe oxides. Arsenite formed both inner- and outer-sphere surface complexes on amorphous Fe oxide and outer-sphere surface complexes on amorphous Al oxides.

In this study, the infrared spectrum was used to examine arsenate adsorption by Yunnan red soil 4 (see Figure 4). It can be seen in Figure 4 that the band intensities of infrared spectra before and after arsenate adsorption by Yunnan red soil 4 were significantly different, indicating that red soil samples before and after adsorption have differences in composition. In the research of iron hydroxide arsenic adsorption and precipitation mechanisms, Liu [29] found that the infrared spectra of hydroxide solid samples before and after arsenic adsorption had $-\text{OH}$ bending vibration absorption bands at $1625\sim 1641\text{ cm}^{-1}$, indicating that the arsenate ion might exist on the red soil surface in the form of protonated bidentate surface complexation of $-\text{FeO}_2\text{As}(\text{O})(\text{OH})^-$ and $-\text{FeO}_2\text{As}(\text{O})^{2-}$. In this study, the infrared spectra also have a $1641\sim 1686\text{ cm}^{-1}$ characteristic absorption band, indicating that re-coordination occurred between the arsenate and the hydroxyl or hydrated base in

the metal oxides, combined on the surface of soil particles via coordination bonds. At the same time, Liu [29] also found that when the initial arsenic concentration was 500 mmol/L, the ferric hydroxide solid after adsorption showed characteristic bands at wavenumber 821.54 cm^{-1} , while adsorption appeared at wavenumber 806.11 cm^{-1} for the arsenic initial concentration of 50 mmol/L. Jia's [30] research found that when pH was 3, the arsenic precipitated as ferric arsenate on the surface of ferric hydroxide, and infrared spectrum analysis showed that the As–O stretching vibration band was at approximately 825 cm^{-1} . It can be seen from the previous study results that the As–O stretching vibration band was at approximately 825 cm^{-1} and decreased with decreasing arsenic concentration. In this study, the arsenic initial concentration was low (0.1 mmol/L), with complex soil particle composition, and the metal oxide content was much lower than the pure product, so less ferric arsenate was formed. The As–O stretching vibration band reduces to 793.68 cm^{-1} in Figure 4. The results show that arsenate formed a small amount of metal arsenide on the red soil surface, which was consistent with previous findings.

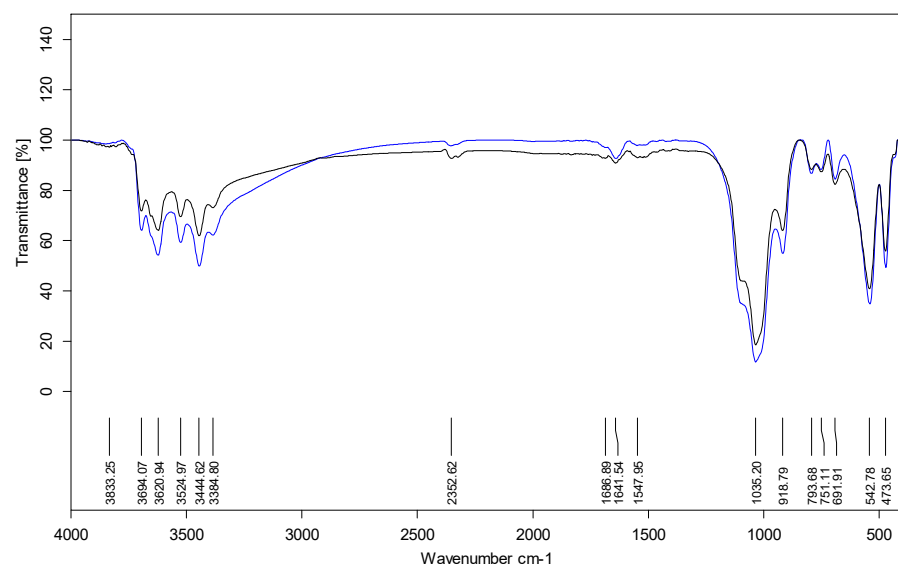


Figure 4. IR Spectra of Red Soil 1 Before and After Arsenate Adsorption.

SEM observation was conducted to elucidate the surface morphology of Yunnan red soil 4 after adsorbing arsenate. As can be seen in Figure 5, a precipitate, similar to a well-knitted net was separated from the water after adsorption of the arsenate, thus revealing excellent adsorption performance.

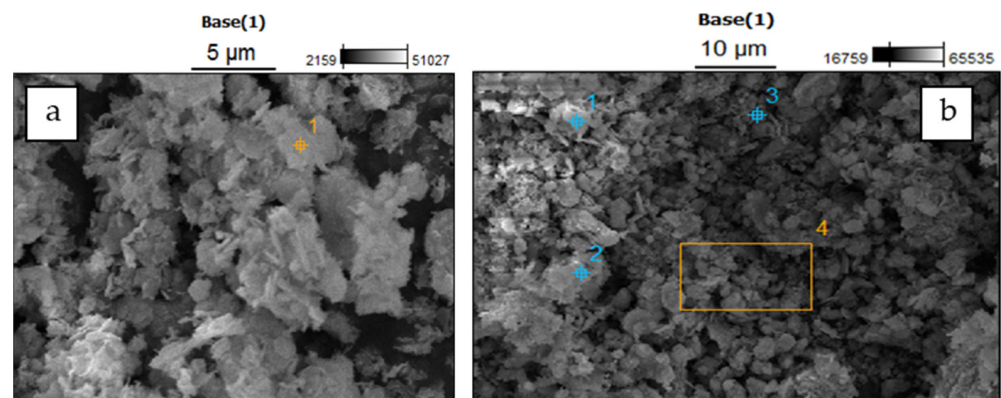


Figure 5. SEM Images of Red Soil 1 Before (a) and After (b) Adsorbing Arsenate.

Our previous studies examined [31] the absorption near-edge structure of arsenic speciation in size-fractions of red soil particles by X-ray. The results indicated that the

concentration of arsenic inversely increased with particle size and was positively correlated with the concentrations of Fe and Al oxides and the specific surface area of the particles. The proportion of non-specifically absorbed As was less than 0.6% in all size fractions, while that of specifically-bound forms varied from 25.0 to 38.5%, based on chemical extraction. The proportion of As species associated with hydrous oxides and stable residual arsenic increased inversely with particle size, within the ranges of 31.0–50.8% and 17.8–40.2%, respectively. The XANES spectra of arsenic adsorbed to the particles were linearly fitted with ferrihydrite, goethite, and amorphous iron oxides, and the results showed that arsenate fractions of 1–5 μm and <1 μm were mainly associated with ferrihydrite and goethite. These findings are consistent with the results of our mechanism studies.

4. Conclusions

Arsenic is highly toxic to most living organisms and is a known human carcinogen. Therefore, the efficient treatment of arsenate-contaminated water is essential. In this study, Yunnan red soil, which was chosen as a sorbent, was successfully applied to remove arsenate from aqueous solutions. The key influencing factors were investigated. The optimal soil/solution ratio was found to be 0.05 g/100 mL, and an optimal shaking speed for the red soil was found to be 225 rpm. The adsorption capacity of Yunnan red soil increased, and the removal rate of arsenate decreased with increasing initial arsenate concentration. The IR spectra of the precipitates further confirmed that the metal arsenide was settled by the Yunnan red soil, indicating that the arsenate ion existed on the red soil surface in the form of protonated bidentate surface complexation of $-\text{FeO}_2\text{As}(\text{O})(\text{OH})^-$ and $\text{FeO}_2\text{As}(\text{O})^{2-}$.

The data obtained indicate that the Yunnan red soil used in this study has excellent potential for use as an unconventional adsorbent that is comparable with commonly used pure chemical adsorbents for As removal, and it may well be suitable as a new adsorbent for As removal during water treatment. More detailed adsorption mechanisms and the release process of As from the sediment should be further examined in future studies.

Author Contributions: Conceptualization, methodology, M.G., W.G. and W.W.; data curation, M.G. and L.S.; writing—original draft preparation, M.G.; writing—review and editing, W.W.; supervision, W.W.; project administration, W.W.; funding acquisition, L.S. and W.W. All authors have read and agreed to the published version of the manuscript.

Funding: This research was supported by the Major Science and Technology Program for Water Pollution Control and Treatment (No. 2010ZX07212-007).

Data Availability Statement: Not applicable.

Conflicts of Interest: The authors declare no conflict of interest.

References

1. Zhang, J.; Ding, T.; Zhang, C. Biosorption and toxicity responses to arsenite (As[III]) in *Scenedesmus quadricauda*. *Chemosphere* **2013**, *92*, 1077–1084. [[CrossRef](#)]
2. Jomova, K.; Jenisova, Z.; Feszterova, M.; Baros, S.; Liska, J.; Hudecova, D.; Rhodes, C.J.; Valko, M. Arsenic: Toxicity, oxidative stress and human disease. *J. Appl. Toxicol.* **2011**, *31*, 95–107. [[CrossRef](#)] [[PubMed](#)]
3. WHO. *Guidelines for Drinking-Water Quality*, 4th ed.; WHO: Geneva, Switzerland, 2011.
4. Jack, C.; Wang, J.; Shraim, A. A global healthy problem caused by arsenic from natural sources. *Chemosphere* **2003**, *52*, 1353–1359. [[CrossRef](#)]
5. Yean, S.; Cong, L.; Yavuz, C.; Mayo, J.; Yu, W.; Kan, A.; Colvin, V.; Tomson, M. Effect of magnetite particle size on adsorption and desorption of arsenite and arsenate. *J. Mater. Res.* **2005**, *20*, 3255–3264. [[CrossRef](#)]
6. Gupta, A.; Yunus, M.; Sankararamkrishnan, N. Zerovalent iron encapsulated chitosan nanospheres—A novel adsorbent for the removal of total inorganic Arsenic from aqueous systems. *Chemosphere* **2012**, *86*, 150–155. [[CrossRef](#)]
7. Darrell, K.N. Worldwide occurrences of arsenate in groundwater. *Science* **2002**, *296*, 2143–2145. [[CrossRef](#)]
8. Hashim, K.S.; AlKhaddar, R.; Shaw, A.; Kot, P.; Al-Jumeily, D.; Alwash, R.; Aljefery, M.H. Electrocoagulation as an Eco-Friendly River Water Treatment Method. *Adv. Water Resour. Eng. Manag.* **2020**, *39*, 219–235. [[CrossRef](#)]
9. Usman, M.; Zarebanadkouki, M.; Waseem, M.; Katsoyiannis, I.A.; Ernst, M. Mathematical modeling of arsenic(V) adsorption onto iron oxyhydroxides in an adsorption-submerged membrane hybrid system. *J. Hazard. Mater.* **2020**, *400*, 123221. [[CrossRef](#)] [[PubMed](#)]

10. Kanel, S.; Greneche, J.; Choi, H. Arsenic(V) Removal from Groundwater Using Nano Scale Zero-Valent Iron as a Colloidal Reactive Barrier Material. *Environ. Sci. Technol.* **2006**, *40*, 2045–2050. [[CrossRef](#)] [[PubMed](#)]
11. Dinesh, M.; Charles, U.; Pittman, J. Arsenic removal from water/wastewater using adsorbents—A critical review. *J. Hazard. Mater.* **2007**, *142*, 1–53. [[CrossRef](#)]
12. Luo, L.; Zhang, S.; Ma, Y. Advance in Research on Arsenic Sorption and Its Affecting Factors in Soils. *Soils* **2008**, *40*, 351–359. [[CrossRef](#)]
13. Feng, Q.; Zhang, Z.; Chen, Y.; Liu, L.; Zhang, Z.; Chen, C. Adsorption and Desorption Characteristics of Arsenic on Soils: Kinetics, Equilibrium, and Effect of Fe(OH)₃ Colloid, H₂SiO₃ Colloid and Phosphate. *Procedia Environ. Sci.* **2013**, *18*, 26–36. [[CrossRef](#)]
14. Hashim, K.S.; Ewadh, H.M.; Zubaidi, S.L.; Kot, P.; Muradov, M.; Aljefery, M.; Al-Khaddar, R. Phosphate removal from water using bottom ash: Adsorption performance, coexisting anions and modelling studies. *Water Sci. Technol.* **2021**, *83*, 77–89. [[CrossRef](#)] [[PubMed](#)]
15. Glass, S.; Mantel, T.; Appold, M.; Sen, S.; Usman, M.; Ernst, M.; Filiz, V. Amine-Terminated PAN Membranes as Anion-Adsorber Materials. *Chem. Ing. Tech.* **2021**, *93*, 1396–1400. [[CrossRef](#)]
16. Khan, S.U.; Farooqi, I.H.; Usman, M.; Basheer, F. Energy Efficient Rapid Removal of Arsenic in an Electrocoagulation Reactor with Hybrid Fe/Al Electrodes: Process Optimization Using CCD and Kinetic Modeling. *Water* **2020**, *12*, 2876. [[CrossRef](#)]
17. Usman, M.; Katsoyiannis, I.; Mitrakas, M.; Zouboulis, A.; Ernst, M. Performance Evaluation of Small Sized Powdered Ferric Hydroxide as Arsenic Adsorbent. *Water* **2018**, *10*, 957. [[CrossRef](#)]
18. Agnieszka, A.; Weronika, S.C.; Grzegorz, J. Arsenate Adsorption on Fly Ash, Chitosan and Their Composites and Its Relations with Surface, Charge and Pore Properties of the Sorbents. *Materials* **2020**, *13*, 5381. [[CrossRef](#)]
19. Wang, Z.; He, B.; Pan, X. Levels, trends and risk assessment of arsenic pollution in Yangzonghai Lake, Yunnan Province, China. *Sci. China Chem.* **2012**, *53*, 1809–1817. [[CrossRef](#)]
20. Hamayun, M.; Mahmood, T.; Naeem, A. Equilibrium and kinetics studies of arsenate adsorption by FePO₄. *Chemosphere* **2014**, *99*, 207–215. [[CrossRef](#)]
21. Zhang, Z.; Wang, P.; Zhang, J.; Xia, S. Removal and mechanism of Cu (II) and Cd (II) from aqueous single-metal solutions by a novel biosorbent from waste-activated sludge. *Environ. Sci. Pollut. Res.* **2014**, *21*, 10823–10829. [[CrossRef](#)] [[PubMed](#)]
22. Tang, W.; Li, Q.; Gao, S.; Shang, J. Arsenic (III, V) removal from aqueous solution by ultrafine α -Fe₂O₃ nanoparticles synthesized from solvent thermal method. *J. Hazard. Mater.* **2011**, *192*, 131–138. [[CrossRef](#)] [[PubMed](#)]
23. Arai, Y.; Sparks, D.; Davis, J. Arsenate adsorption mechanisms at the allophone-water interface. *Environ. Sci. Technol.* **2005**, *39*, 2537–2544. [[CrossRef](#)] [[PubMed](#)]
24. Vu, T.; Le, G.; Dao, C.; Dang, L.; Nguyen, K.; Nguyen, Q.; Dang, P.; Tran, H.; Duong, Q.; Nguyen, T.; et al. Arsenic removal from aqueous solutions by adsorption using novel MIL-53(Fe) as a highly efficient adsorbent. *RSC Adv.* **2015**, *5*, 5261–5268. [[CrossRef](#)]
25. Huang, C. *Soil Science*; China Agriculture Press: Beijing, China, 2000; pp. 169–170.
26. Zhu, J.; Pigna, M.; Cozzolino, V.; Caporale, A.G.; Violante, A. Sorption of arsenite and arsenate on ferrihydrite: Effect of organic and inorganic ligands. *J. Hazard. Mater.* **2011**, *189*, 564–571. [[CrossRef](#)]
27. Wang, S.; Mulligan, C. Natural attenuation processes for remediation of arsenic contaminated soils and groundwater. *J. Hazard. Mater.* **2006**, *138*, 459–470. [[CrossRef](#)]
28. Goldberg, S.; Johnston, C. Mechanisms of arsenic adsorption on amorphous oxides evaluated using macroscopic measurements, vibrational spectroscopy, and surface complexation modeling. *J. Colloid Interface Sci.* **2001**, *234*, 204–216. [[CrossRef](#)]
29. Liu, H.L.; Liang, M.; Zhu, Y.; Cai, F.; Zou, H. The Adsorption of Arsenic by Ferric Hydroxide and its Precipitation Mechanism. *Acta Sci. Circumstantiae* **2009**, *29*, 1011–1020.
30. Jia, Y.; Xu, L.; Fang, Z.; Demopoulos, G. Demopoulos. Observation of surface precipitation of arsenate on ferrihydrite. *Environ. Sci. Technol.* **2006**, *40*, 3248–3253. [[CrossRef](#)]
31. Li, S.; Luo, Y.; Zhang, H.; Haung, J.; Li, Z.; Wei, J. Arsenic forms in various particle-size fractions of red soil-Chemical fractionation and speciation using XANES analysis. *Acta Sci. Circumstantiae* **2011**, *31*, 2733–2739. [[CrossRef](#)]